

# Observation of $\alpha$ and $\gamma$ Crystal Forms and Amorphous Regions of Nylon 6–Clay Nanocomposites Using Solid-State $^{15}\text{N}$ Nuclear Magnetic Resonance

Lon J. Mathias,\* Rick D. Davis, and William L. Jarrett

University of Southern Mississippi,  
School of Polymers and High Performance Materials,  
Hattiesburg, Mississippi 39406-0076

Received August 5, 1999

Revised Manuscript Received September 24, 1999

**Introduction.** Recently, clay–polymer nanocomposites obtained from surface-treated montmorillonite have attracted enormous interest because of unexpectedly high property enhancements at low clay content (1–5 wt %). For instance, improved heat distortion temperatures, moduli, tensile strengths, and yield stresses have been reported for nanocomposites with <5 wt % clay in nylon 6,<sup>1–7</sup> poly(*N*-vinylcarbazole),<sup>8</sup> polypropylene,<sup>9</sup> polyester,<sup>10–13</sup> polyimide,<sup>14–17</sup> poly(methyl methacrylate),<sup>18</sup> poly(ethylene oxide),<sup>19–21</sup> poly(ether–amine),<sup>22,23</sup> polystyrene,<sup>24</sup> and polyurethane.<sup>25,26</sup> The improved properties are believed to result from synergistic interactions between high surface area clay particles and the polymer. The nature, origin, and strength of these interactions are not well understood. Spectroscopic efforts to evaluate the effects of clay on the polymer have combined infrared spectroscopy (IR),<sup>6,11</sup> thermal analysis, and X-ray diffraction (XRD).<sup>1–26</sup> These techniques have shown that clay induces the  $\gamma$  crystal phase in nylon 6 while maintaining about the same percent crystallinity. However, no determination has been made of whether this phase exists alone or whether it is a kinetically formed component that slowly relaxes to the more stable  $\alpha$ -crystal form.

We previously reported the observation of  $\alpha$ ,  $\gamma$ , and amorphous phases in nylon 6 using solid-state  $^{15}\text{N}$  CP/MAS NMR.<sup>27</sup> Because of speed, simplicity, and accuracy, this method has been used by us and others for characterization of crystallinity in a variety of homo- and copolyamides.<sup>17–33</sup> In an attempt to better understand the interaction between exfoliated clay and nylon, we have applied solid-state  $^{15}\text{N}$  CP/MAS NMR methods to characterization of typical nylon 6–clay nanocomposites. We report our initial results here.

**Experimental Section.** 12-Aminolauric acid treated montmorillonite was used as received from Nanocor, Inc.<sup>34</sup> The cation exchange capacity (CEC) was ca. 119 mequiv/100 g of montmorillonite as reported on the MSDS.<sup>34</sup>

Solid-state  $^{15}\text{N}$  CP/MAS NMR spectra were collected on a Bruker MSL-400 MHz NMR operating at 40.57 MHz spectral frequency. A routine  $^{15}\text{N}$  CP/MAS pulse program was used with a 7.8  $\mu\text{s}$ , 90° pulse width and a 1 ms contact time. The average number of scans was 30 000 for the nanocomposite and 21 000 for the commercial nylon 6. Chemical shifts are reported relative to  $^{15}\text{N}$ -labeled glycine at 0 ppm.

Nylon 6 and nanocomposite samples for solution  $^{13}\text{C}$  NMR were prepared by dissolving in trifluoroethanol (TFE) with heating and then adding  $\text{CDCl}_3$  to the cooled solution to give a sample with 10 wt % polymer in a

solvent consisting of 80:20 TFE to  $\text{CDCl}_3$ . Solution spectra were collected on an Aspect AC-300 MHz NMR operating at 75.4 MHz spectral frequency. A 5 mm NMR probe was used with the average number of transients being 15 000 to give sufficient signal-to-noise to allow quantitation of end groups<sup>35</sup> and cis-amide content.<sup>36</sup>

The nylon 6–clay nanocomposite was synthesized following the procedure reported by Kurachi and co-workers at Toyota.<sup>2</sup> A 2 L Parr reactor was charged with  $\epsilon$ -caprolactam (73.9 g, 0.65 mol) and montmorillonite that had been treated with 12-aminolauric acid to give a clay to amino acid ratio of 3.65 g to 0.77 g (0.066 mol). The vessel was purged with nitrogen for 25 min and then sealed. The temperature was raised to 110 °C, and the vessel was again purged with nitrogen for 30 s. The reactor was sealed again and the temperature raised to 250 °C under a nitrogen atmosphere. The reaction proceeded for 2 days with slow stirring. The molten nanocomposite was isolated by pouring into cold water, filtering, and drying at 70 °C for 24 h at 0.1 mmHg. The nanocomposite was a hard, brown material. A portion of the product was dissolved in TFE, reprecipitated into methanol, and dried under vacuum at room temperature to remove residual monomer. The reprecipitated nanocomposite was beige and flaky. Samples of commercial nylon 6 and the nylon 6–clay nanocomposite were annealed at 200 °C for 12 h at 0.1 mmHg and then slowly cooled to room temperature under vacuum.

**Results and Discussion.** Number-average molecular weights along with residual monomer, acid, and amine end group contents and cis-amide conformer contents were calculated using peak intensities from solution  $^{13}\text{C}$  NMR spectra of the nylon 6 and nylon 6–clay nanocomposite. A solution  $^{13}\text{C}$  NMR spectrum of the nylon 6–clay nanocomposite is provided in Figure 1. Complete peak assignments will be reported in a forthcoming publication; partial assignments have been reported.<sup>36</sup> The peaks used for calculations were the  $\text{CH}_2$ 's in nylon 6 that were  $\alpha$  to the amine end group,  $\alpha$  to the acid end group, and  $\alpha$  to the nitrogen of the cis-amide, and  $\text{CH}_2$ 's in residual caprolactam that were  $\alpha$  to the nitrogen of the amide (Figure 2). Calculated values were 5 wt % residual caprolactam, 1.7 wt % cis-amide, conformers, 1.2 wt % acid end groups, and 19 100 g/mol molecular weight. These values are similar to those observed for commercial nylon 6, except that the molecular weight was slightly higher. Interestingly, no neutral amine end groups were observed for the nanocomposite by solution NMR, apparently because most or all of amine end groups were protonated or ionically bound to the clay surface.

Taking into account the residual caprolactam, a theoretical molecular weight of 20 000 g/mol was calculated on the basis of the assumption that all the 12-aminolauric acid on the clay surface was available as the initiating species, i.e., one 12-aminolauric acid group per polymer molecule. This molecular weight is very close to the actual value estimated by NMR and was consistent with high conversion acid-catalyzed ring-opening polymerization of nylon 6 initiated by the 12-aminolauric acid. On the basis of these results, we conclude that all of the nylon amine end groups are protonated and bound to the clay surface. Thus, their

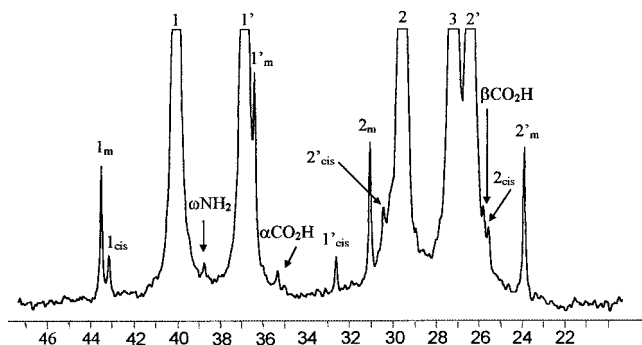


**Figure 1.** Solution  $^{13}\text{C}$  NMR of nylon 6-clay nanocomposite: expansion of aliphatic region with trans-amide conformer peaks off scale (peak assignments as in Figure 2); "cis" indicates peaks for the cis-amide conformer.

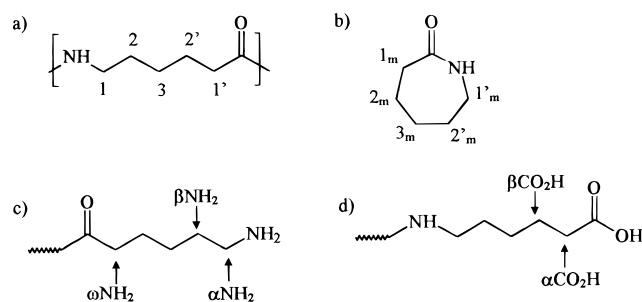


**Figure 2.** Chemical structure and  $^{13}\text{C}$  NMR identifications of (a) nylon 6, (b)  $\epsilon$ -caprolactam, (c) amine end group, and (d) acid end group.

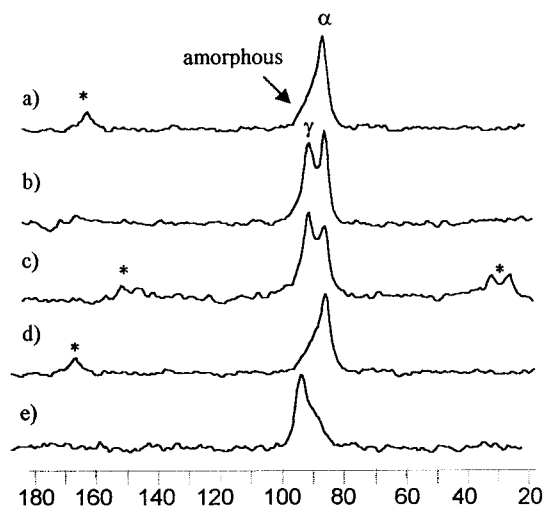


**Figure 3.** Solid-state  $^{15}\text{N}$  CP/MAS NMR of (a) nylon 6, (b) nylon 6-clay nanocomposite, (c) reprecipitated nylon 6-clay nanocomposite, (d) annealed nylon 6, and (e) annealed nylon 6-clay nanocomposite. Asterisk indicates spinning sidebands.

chemical shifts would be very different from the neutral amine end groups normally observed in nylon 6. We did observe a peak at 38.4 ppm that was the same intensity as the peak assigned to the  $\alpha$ -CH<sub>2</sub> to the acid end groups. In fact, when a trace of acid was added to the commercial nylon 6 NMR solution, the amine  $\alpha$ -CH<sub>2</sub> peak moved from 40.7 to 38.4 ppm, confirming that the peak at 38.4 ppm is due to the  $\alpha$ -CH<sub>2</sub> to the protonated amine end groups while the chemical shift of the  $\alpha$ -CH<sub>2</sub> to the acid end group remained unchanged.

Figure 3 compares the solid-state  $^{15}\text{N}$  CP/MAS spectra of the nylon 6 and nylon 6-clay nanocomposite. The peaks were assigned to the  $\alpha$ ,  $\gamma$ , and amorphous phases of nylon 6 on the basis of values reported in several

papers.<sup>27-33</sup> The  $\alpha$  phase is normally the favored of the two crystal structures; thus, the  $\alpha$  and amorphous phases are generally the only phases observed in nylon 6. The  $\gamma$  phase can be induced using various solvent treatments and thermal history. Since the  $\alpha$  phase is thermodynamically favored, annealing most nylon samples at temperatures near the melting point produces only  $\alpha$  and amorphous phases. The  $^{15}\text{N}$  CP/MAS NMR spectra of nylon 6 (Figure 3a) contained one sharp peak at 84.9 ppm with a significant broad absorption between 77 and 95 ppm. The broad component is due to the amorphous phase and the sharp peak to the  $\alpha$  crystal phase.<sup>27-30,32,33</sup> The spectra of the nylon 6-clay nanocomposites (b and c) each exhibited two sharp peaks at 89.3 and 84.9 ppm and a broad peak spanning this range. The sharp peak at 89.3 ppm is assigned to the  $\gamma$  crystal phase. Clearly, the nylon 6 in the presence of high surface area clay particles adopts both  $\alpha$  and  $\gamma$  crystal phases in about equal amounts. Since only the  $\alpha$  phase was observed in the commercial nylon 6, the presence of the  $\gamma$  phase in the nanocomposite must result from interaction with clay. This suggests that clay stabilizes or/and induces the  $\gamma$  phase of nylon 6, even after solvent reprecipitation.

Annealing the nanocomposites under conditions that generally give only the  $\alpha$  crystal phase further supported this assumption. The solid-state  $^{15}\text{N}$  CP/MAS spectra of nylon 6 (Figure 3a) and the nylon 6-clay nanocomposite (b and c) were compared to their annealed analogues (d and e, respectively). Annealing nylon 6 at 200 °C under vacuum followed by slow cooling caused no change in the  $\alpha$  crystal and amorphous phases, while annealing the nylon 6-clay nanocomposite under the same conditions produced only the  $\gamma$  crystal and amorphous phases. Since no  $\alpha$  phase was observed in the latter sample, the clay has completely altered the morphology of the nylon 6 even at ca. 5 wt % incorporation. One of two possibilities exists. Either the clay surface induces kinetically favored formation of the  $\gamma$ -crystal form, or it changes the thermodynamics of the system such that the  $\gamma$ -crystal form is more stable even at nanometer distances from the clay surface. Since the latter is unlikely, we believe that kinetics is the controlling factor. That is, because the amine end groups are tightly bound to the clay surface, but not arrayed on the surface at an interchain distance that allows formation of the layered hydrogen-bonded sheets of the  $\alpha$ -form, the  $\gamma$ -form is generated by default. How this crystal form develops or propagates at large distances away from the surface and how this overall morphology so drastically effects thermal and physical properties are questions we are attempting to answer using a variety of solid-state NMR methods. It is clear, however, that basic changes in the molecular organization induced by the clay surface dramatically alter the macroscopic properties.

**Acknowledgment.** We gratefully acknowledge Nanocor, Inc., of Arlington Heights, IL, for providing montmorillonite samples.

## References and Notes

- (1) Kojima, Y.; Usuki, A.; Kawasumi, M.; Okada, A.; Kurauchi, T.; Kamigaito, O. One-Pot Synthesis of Nylon 6-Clay Hybrid. *J. Polym. Sci., Part A: Polym. Chem.* **1993**, *31*, 1775.
- (2) Kurauchi, T.; Okada, A.; Nomura, T.; Nishio, T.; Saegusa, S.; Deguchi, R. Nylon 6-Clay Hybrid—Synthesis, Properties

- and Application to Automotive Timing Belt Cover. Japanese Pat. 910584, 1991.
- (3) Kojima, Y.; Usuki, A.; Kawasumi, M.; Okada, A.; Kurauchi, T.; Kamigaito, O.; Kaji, K. Novel Preferred Orientation in Injection-Molded Nylon 6-Clay Hybrid. *J. Polym. Sci., Part B: Polym. Phys.* **1995**, *33*, 1039.
  - (4) Liu, L.; Qi, Z.; Zhu, X. Studies on Nylon 6/Clay Nanocomposites by Melt-Intercalation Process. *J. Appl. Polym. Sci.* **1999**, *71*, 1133.
  - (5) Kojima, Y.; Usuki, A.; Kawasumi, M.; Okada, A.; Kurauchi, T.; Kamigaito, O. Mechanical Properties of Nylon 6-Clay Hybrid. *J. Mater. Res.* **1993**, *8*, 1185.
  - (6) Usuki, A.; Kojima, Y.; Kawasumi, M.; Okada, A.; Fukushima, Y.; Kurauchi, T.; Kamigaito, O. Synthesis of Nylon 6-Clay Hybrid. *J. Mater. Res.* **1993**, *8*, 1179.
  - (7) Kojima, Y.; Usuki, A.; Kawasumi, M.; Okada, A.; Kurauchi, T.; Kamigaito, O.; Kaji, K. Fine Structure of Nylon 6-Clay Hybrid. *J. Polym. Sci., Part B: Polym. Phys.* **1994**, *32*, 625.
  - (8) Biswas, M.; Ray, S. Preparation and Evaluation of Composites from Montmorillonite and Some Heterocyclic Polymers. 1: Poly(N-vinylcarbazole)-Montmorillonite Nanocomposite System. *Polymer* **1998**, *39*, 6423.
  - (9) Kawasumi, M.; Hasegawa, N.; Kato, M.; Usuki, A.; Okada, A. Preparation and Mechanical Properties of Polypropylene-Clay Hybrids. *Macromolecules* **1997**, *30*, 6333.
  - (10) Kornmann, X.; Berglund, L. A.; Sterte, J.; Giannelis, E. P. Nanocomposites Based on Montmorillonite and Unsaturated Polyester. *Polym. Eng. Sci.* **1998**, *38*, 1351.
  - (11) Ismail, M. R.; Ali, M. A. M.; El-Milligy, A.; Afifi, M. S. Studies of Sand/Clay Unsaturated Polyester Composite Materials. *J. Appl. Polym. Sci.* **1999**, *72*, 1031.
  - (12) Ke, Y.; Long, C.; Qi, Z. Crystallization, Properties, and Crystal and Nanoscale Morphology of PET-Clay Nanocomposite. *J. Appl. Polym. Sci.* **1999**, *71*, 1139.
  - (13) Messersmith, P. B.; Giannelis, E. P. Polymer-Layered Silicate Nanocomposites: In Situ Interactive Polymerization of Caprolactone in Layered Silicates. *Chem. Mater.* **1993**, *5*, 1064.
  - (14) Padmanada, T.; Kaviratna, D.; Pinnavaia, T. On the Nature of Polyimide-Clay Hybrid Composites. *Chem. Mater.* **1994**, *6*, 573.
  - (15) Yano, K.; Usuki, A.; Okada, A.; Kurauchi, T.; Kamigaito, O. Synthesis and Properties of Polyimide-Clay Hybrid. *J. Polym. Sci., Part A: Polym. Chem.* **1993**, *31*, 2493.
  - (16) Yano, K.; Usuki, A.; Okada, A. Synthesis and Properties of Polyimide-Clay Hybrid Films. *J. Polym. Sci., Part A: Polym. Chem.* **1997**, *35*, 2289.
  - (17) Zhu, Z.; Yang, Y.; Yin, J.; Wang, X.; Ke, Y.; Qi, Z. Preparation and Properties of Organosoluble Montmorillonite/Polyimide Hybrid Materials. *J. Appl. Polym. Sci.* **1999**, *73*, 2063.
  - (18) Chen, G.; Yao, K.; Zhao, J. Montmorillonite Clay/Poly(methyl methacrylate) Hybrid Resin and Its Barrier Property to the Plasticizer Within Poly(vinyl chloride) Composite. *J. Appl. Polym. Sci.* **1999**, *73*, 425.
  - (19) Mekhamer, W. K.; Assad, F. F. Flocculation and Coagulation of Ca- and K-Saturated Montmorillonite in the Presence of the Poly(ethylene oxide). *J. Appl. Polym. Sci.* **1999**, *73*, 659.
  - (20) Ruiz-Hitzky, E. Conducting Polymers Intercalated in Layered Solids. *Adv. Mater.* **1993**, *5*, 334.
  - (21) Ruiz-Hitzky, E.; Aranda, P.; Casal, B.; Galvan, J. Nanocomposite Materials with Controlled Ion Mobility. *Adv. Mater.* **1995**, *7*, 180.
  - (22) Lan, T.; Pinnavaia, T. Clay-Reinforced Epoxy Nanocomposites. *Chem. Mater.* **1994**, *6*, 2216.
  - (23) Shi, H.; Lan, T.; Pinnavaia, T. Interfacial Effects on the Reinforcement Properties of Polymer-Organoclay Nanocomposites. *Chem. Mater.* **1996**, *8*, 1584.
  - (24) Noh, M. W.; Lee, D. C. Synthesis and Characterization of PS-Clay Nanocomposite by Emulsion Polymerization. *Polym. Bull.* **1999**, *42*, 619.
  - (25) Wang, Z.; Pinnavaia, T. J. Nanolayer Reinforcement of Elastomeric Polyurethane. *Chem. Mater.* **1998**, *10*, 3769.
  - (26) Chen, T. K.; Tien, Y. I.; Wei, K. H. Synthesis and Characterization of Novel Segmented Polyurethane/Clay Nanocomposite via Poly( $\epsilon$ -caprolactone)/Clay. *J. Polym. Sci., Part A: Polym. Chem.* **1999**, *37*, 2225.
  - (27) Powell, D. G.; Mathias, L. J. Characterization of Nylon 6 by  $^{15}\text{N}$  Solid-State Nuclear Magnetic Resonance. *J. Am. Chem. Soc.* **1990**, *112*, 669.
  - (28) Hatfield, G.; Glans, J.; Hammond, W. Characterization of Structure and Morphology in Nylon 6 by Solid-State  $^{13}\text{C}$  and  $^{15}\text{N}$  NMR. *Macromolecules* **1990**, *23*, 1654.
  - (29) Powell, D. G.; Mathias, L. J.; Autran, J. P.; Porter, R. S. Solid State  $^{15}\text{N}$  Nuclear Magnetic Resonance of  $^{15}\text{N}$ -labeled Nylon 6 and Nylon 11: Observation of Multiple Crystalline Forms and Amorphous Regions. *Mater. Sci. Eng.* **1990**, *126*, 253.
  - (30) Johnson, C. G.; Mathias, L. J. Nylon 13,13 Analysis by X-ray and Solid State NMR Treatment-Dependent Crystal Forms. *Polymer* **1993**, *34*, 4978.
  - (31) Johnson, C. G.; Mathias, L. J. Solid-State NMR Investigation of Nylon 12. *Macromolecules* **1991**, *24*, 6114.
  - (32) Johnson, C. G.; Cypcar, C. C.; Mathias, L. J.  $^{13}\text{C}$  and  $^{15}\text{N}$  Solid-State NMR of Copolymers of Nylon 6 and 7: Observation of a Stable Pseudo-hexagonal Phase. *Macromolecules* **1995**, *28*, 8535.
  - (33) Johnson, C. G.; Mathias, L. J. Solid-State NMR Characterization of Copolymers of Nylon 11 and Nylon 12. *Solid State Nucl. Magn. Reson.* **1997**, *8*, 161.
  - (34) Nanacor, Inc., 1500 West Shure Drive, Arlington Heights, IL 60004-7803.
  - (35) Description of quantifying end groups in nylon 6 will be reported in a forthcoming publication.
  - (36) Steadman, S. J.; Mathias, L. J. A New Non-acidic Mixed Solvent System for Nylon Nuclear Magnetic Resonance: Cis-Amide Quantitation in Nylons and Model Amides. *Polymer* **1997**, *38*, 5297.

MA991307P